Journal of Communications and Information Networks, Vol.2, No.4, Dec. 2017
DOI: 10.1007/s41650-017-0038-2

Research paper

Special Focus on Optical Wireless Communication

Position encoded asymmetrically clipped optical orthogonal frequency division multiplexing in visible light communications

Osama Saied[1], Zabih Ghassemlooy[1,3*], Xuan Tang[2], Xuewu Dai[1], Hoa Le Minh[1], Bangjiang Lin[1]

1. Optical Communications Research Group, NCRLab, Faculty of Engineering and Environment, Northumbria University, Newcastle Upon Tyne NE18ST, UK
2. Quanzhou Institute of Equipment Manufacturing, Haixi Institutes, Chinese Academy of Sciences, Quanzhou 350001, China
3. College of Engineering, Huaqiao University, Quanzhou 362021, China

* Corresponding author, Email: z.ghassemlooy@northumbria.ac.uk

Abstract: A PE-ACO-OFDM (Position-Encoded Asymmetrically Clipped Optical Orthogonal Frequency Division Multiplexing) signaling scheme for intensity modulation and direct detection is introduced in this paper, where the anti-asymmetry characteristics of ACO-OFDM are exploited to improve the rate of data transmission. This is achieved by reducing the symbol duration of the ACO-OFDM signal, where only the first half of ACO-OFDM is used to transmit the ACO-OFDM data symbol after inverting its negative samples to positive ones. In addition, encoded ACO-OFDM samples are combined with every ACO-OFDM symbol to allow the receiver to identify the position of the inverted samples. Simulation results are introduced, and it is shown that the data rates of PE-ACO-OFDM improve by 33% compared with ACO-OFDM, when a 256-quadrature amplitude modulation scheme is considered as the encoded constellation order. It is also shown that the signal to noise ratio of the proposed PE-ACO-OFDM is higher by almost 1 dB compared with the traditional ACO-OFDM.

Keywords: visible light communications, ACO-OFDM, anti-asymmetry characterization, symbol duration, data rates

Citation: O. Saied, Z. Ghassemlooy, X. Tang, et al. Position encoded asymmetrically clipped optical orthogonal frequency division multiplexing in visible light communications [J]. Journal of communications and information networks, 2017, 2(4): 1-10.

1 Introduction

VLC (Visible Light Communications) is a unique wireless technology that combines illumination, data transmission, and localization (i.e., deployed mostly indoors). Owing to its utilization of white LEDs (Light Emitting Diodes), VLC has been considered a suitable candidate for future generation communication networks, offering energy efficient service, unregulated frequency spectrum, and a potentially low-cost solution[1,2]. However, standard LEDs, in particular white phosphor-based LEDs, have a low modulation bandwidth, typically in the range of a few MHz, which is considered as a limiting factor for the communication networks' modulation bandwidth. Several approaches have been proposed to tackle this LED bandwidth limitation, and to increase the transmission speed; one of them is blue

Manuscript received May 27, 2017; accepted Jul. 10, 2017
This work is supported by the EPSRC research grant (No. EP/P006299/1).

filtering, in which the slow yellowish component is filtered out, thus increasing the 3 dB bandwidth by up to tens of MHz[3,4]. However, blue filtering causes a reduction in the signal power, which results in a much lower SNR (Signal-to-Noise-Ratio)[5]. Alternatively, pre- and post-equalization schemes both in analogue[6,7] and digital[8,9] domains have been used to increase data rates R_d.

In recent years, utilization of spectrally efficient modulation formats such as OFDM (Orthogonal Frequency Division Multiplexing) has been the focus of increasing attention of researchers, to combat the bandwidth limitations of VLC systems[10].

The main advantage of OFDM is the fact that it offers an effective solution for reducing the ISI (Inter-Symbol Interference) in band-limited systems. Since data transmission occurs in parallel, the symbol period takes a much longer time than in serial data communications with the same R_d. As such, ISI affects at most one symbol, which simplifies the equalization process[11]. Furthermore, the low frequency noise caused by the DC wandering and flickering interference owing to florescent lights was mitigated by not modulating the first OFDM subcarrier[12]. Finally, OFDM can compensate for the performance degradation at frequencies beyond the 3 dB modulation bandwidth by exploiting its bit- and power-loading feature[13]. As such, OFDM is a robust modulation scheme that can support high R_d in VLC systems. For example, a 3 Gb/s VLC system was reported in Ref. [14]. Other VLC systems offering Gb/s data rates using OFDM were also reported in Refs. [15-17]. In IM/DD (Intensity Modulation and Direct Detection) based VLCs, the requirement for the light intensity to be positive and real implies that complex and bipolar signal formats such as the traditional OFDM cannot be used. Thus, DCO-OFDM (DC-biased Optical OFDM) and ACO-OFDM (Asymmetrically Clipped Optical OFDM) were proposed for IM/DD VLC systems[18,19]. Both schemes are constrained to have HS (Hermitian Symmetry) in order to provide real-time domain signals at the cost of 50% of the electrical bandwidth[20].

In DCO-OFDM, to ensure obtaining an all-positive OFDM signal, a DC bias is added to the signal prior to clipping the negative residual signals[20]. However, the application of a large DC bias necessitates the use of a much higher mean optical power. In addition, clipping the negative residual signals also results in clipping the noise signal. In contrast, in ACO-OFDM, only the odd subcarriers are modulated to ensure generating anti-asymmetric time domain signals, thus clipping the negative signals at the zero level without leading to the loss of information. Consequently, ACO-OFDM represents a more efficient scheme in terms of the optical power requirements, compared with OOK (On-Off-Keying), and has a low clipping noise level, whereas DC-OFDM offers a more bandwidth-efficient solution[21].

The un-modulated even ACO-OFDM subcarriers and their anti-symmetric time domain characteristics were investigated in Refs. [22-24] for enhancing the system performance. A trade-off between ACO-OFDM and DC-OFDM was outlined in Ref. [22] where only the odd and even subcarriers were modulated in ACO-OFDM and in DCO-OFDM schemes, respectively. In Ref. [22] both schemes were combined and transmitted simultaneously, where the interference cancelation method was used at the Rx (Receiver) to separate them. A hybrid OOK and ACO-OFDM methodology was introduced in Ref. [23] to increase the spectral efficiency of ACO-OFDM. In this approach, the anti-symmetry feature of the ACO-OFDM time domain signal was exploited, such that the negative ACO-OFDM signals were clipped as in traditional ACO-OFDM to modulate the '0' bits in OOK. While the '1' bits of OOK were modulated by clipping the positive ACO-OFDM time domain signals and adding a DC bias. Furthermore, R_d of ACO-OFDM was increased by almost 33% by reducing the time domain symbol duration where only the first half of ACO-OFDM was transmitted following inversion of negative samples and inserting higher amplitude pilots to allow the receiver to locate the inverted samples[24]. However, since OFDM has a high PAPR (Peak-to-Average Power Ratio), where higher amplitude pilot signals can affect the system's performance when applied

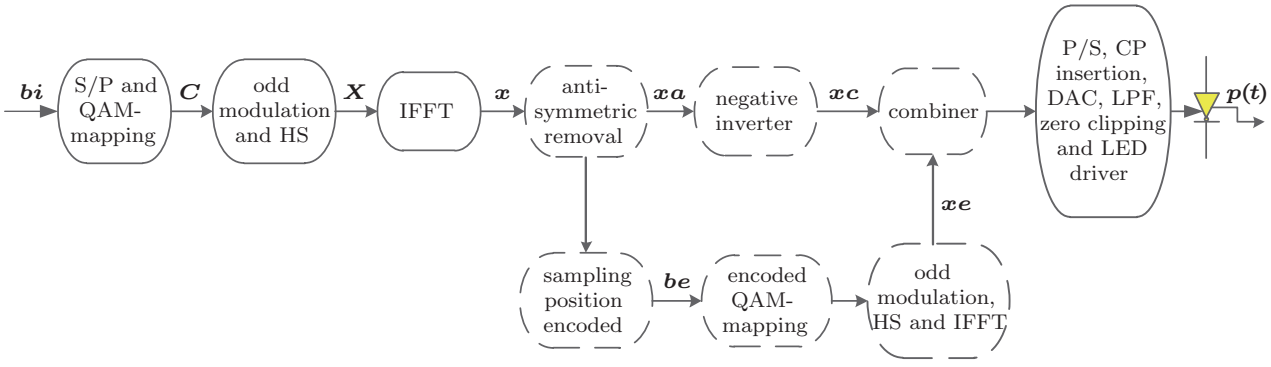

Figure 1 A block diagram of PE-ACO-OFDM Tx

to an LED light source with a limited linear power-current characteristics, in the form of harmonic and intermodulation products.

In this paper, we present a novel OFDM technique in which the advantages of ACO-OFDM with the anti-asymmetric time domain characteristics are exploited in order to increase R_d. This is achieved by reducing the number of transmitted samples per OFDM symbol where the second half of the ACO-OFDM signal is removed and only the first half is used to transmit the ACO-OFDM signal following the inversion of its negative samples. However, additional encoded ACO-OFDM samples are combined with each OFDM symbol to provide the Rx with knowledge of the position of the inverted samples. The results show that with the proposed PE-ACO-OFDM, R_d increases with the increasingly encoded constellation order.

The rest of the paper is organized as follows: section 2 illustrates the system module of the proposed scheme and in section 3, R_d of the proposed scheme is shown and analyzed. The orthogonality of the proposed PE-ACO-OFDM is mathematically shown in section 4. Results obtained from the proposed scheme are analyzed and evaluated in section 5. Finally, conclusions are drawn in section 6.

2 System model

2.1 PE-ACO-OFDM transmitter (Tx)

Fig. 1 shows the block diagram of the proposed PE-ACO-OFDM Tx. As in traditional ACO-OFDM, the serial binary bits $\boldsymbol{bi}$ ($\boldsymbol{bi} \in \{0,1\}$) are converted into parallel streams and then mapped to a complex data vector $\boldsymbol{C}$, given by

$$\boldsymbol{C} = [C_0, C_1, C_2, \cdots, C_{D-1}], \tag{1}$$

where D is the number of transmitted complex data per OFDM symbol. In ACO-OFDM, to meet the requirements of the IM/DD, $\boldsymbol{C}$ must go through odd modulation and HS processes (Fig. 2), where the resulting complex symbol is given by

$$\begin{aligned}\boldsymbol{X} = [&0, C_0, 0, C_1, 0, C_2, \cdots, C_{D-2}, 0, C_{D-1},\\ &0, C^{\star}_{D-1}, 0, C^{\star}_{D-2}, \cdots, C^{\star}_2, 0, C^{\star}_1, 0, C^{\star}_0].\end{aligned} \tag{2}$$

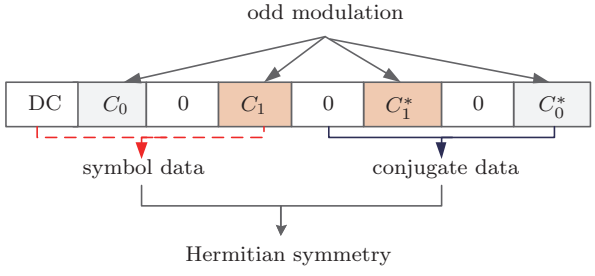

Figure 2 The implementation of odd modulation and HS of ACO-OFDM

An IFFT (Inverse Fast Fourier Transform) is then performed on $\boldsymbol{X}$. Thus, the IFFT output signal $\boldsymbol{x}$ is an anti-symmetric real time domain signal (Fig. 3(a)), which is suitable for IM/DD VLC systems, where $\boldsymbol{x} = \{x_0, x_1, x_2, \cdots, x_{N-1}\}$ and $N = 4D$ is the total number of the time domain samples per OFDM symbol, which is also equal to the IFFT points. As was already mentioned, this anti-symmetric characteristic of the ACO-OFDM time

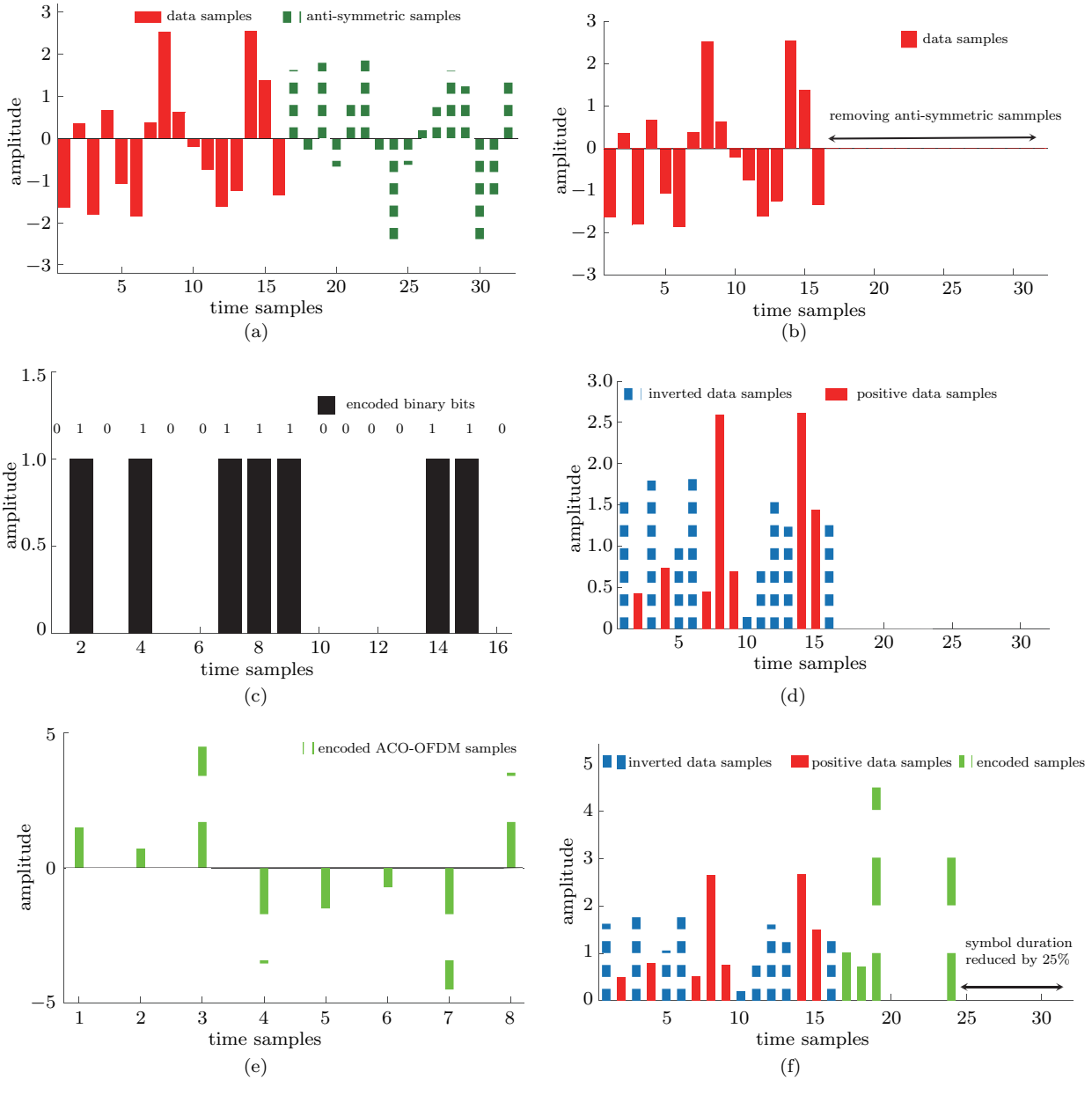

Figure 3 (a) The ACO-OFDM time domain signal $\boldsymbol{x}$, (b) the ACO-OFDM time domain signal after the anti-symmetric removal process $\boldsymbol{xa}$, (c) the encoded negative and positive samples positions $\boldsymbol{be}$, (d) $\boldsymbol{xa}$ following the negative samples inversion process $\boldsymbol{xc}$, (e) the encoded ACO-OFDM signal $\boldsymbol{xe}$, and (f) the combination of $\boldsymbol{xe}$ with $\boldsymbol{xc}$. $N = 32$, $M = 256 - QAM$ and $M_e = 256 - QAM$

domain signal improves the power efficiency compared with DCO-OFDM. On the other hand, the redundant anti-symmetric samples in ACO-OFDM reduce spectral efficiency by a half, compared with DCO-OFDM.

However, to increase the spectral efficiency of ACO-OFDM, additional signal processing modules are included, (Fig. 1, dotted boxes), which are

- Removal of anti-symmetric samples of $\boldsymbol{x}$—where the number of samples in the resulting signal $\boldsymbol{xa}$ (Fig. 3(b)) is now $N/2$ (i.e., $\boldsymbol{xa} = \{xa_0, xa_1, \cdots, xa_{N/2-1}\}$).
- Sampling position encoder—$\boldsymbol{xa}$ is applied to a sampling position encoder to encode the position of its negative and positive samples, i.e., if $xa_j \leqslant 0$, then insert "0", otherwise "1" , where j is the jth

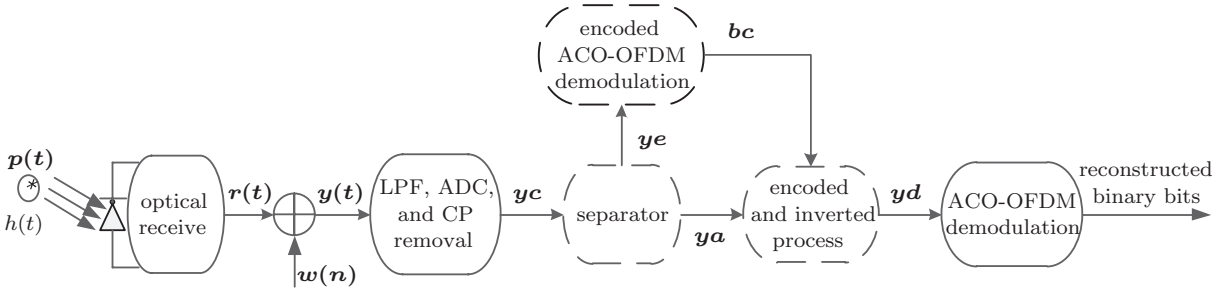

Figure 4 A block diagram of PE-ACO-OFDM Rx

ACO-OFDM sample after anti-symmetric removal process (Fig. 3(c)). Therefore, the resulting encoded binary bits $\boldsymbol{be} \in \{0, 1\}$ have $N/2$ bits.

• ACO-OFDM signal—$\boldsymbol{be}$ is then applied to the following modules of encoded QAM-mapping, odd modulation, HS and IFFT, in order to generate the new ACO-OFDM signal $\boldsymbol{xe}$ (Fig. 3(e)), with $2N/L_e$ number of samples, where $L_e = \text{lb}M_e$ and M_e is the encoded constellation order of QAM (i.e., 4, 8, 16, 32).

• Inverter—the negative samples of $\boldsymbol{xa}$ are inverted (Fig. 3(d)) and combined with $\boldsymbol{xe}$ (Fig. 3(f)).

Finally, as in traditional ACO-OFDM, the resulting combined signal $\boldsymbol{xp}$ passes through a P/S (Parallel to Serial) convertor, a CP (Cyclic Prefix) inserter, a DAC (Digital-to-Analog Convertor), a LPF (Low Pass Filter) and zero clipping modules prior to being biased and used for IM of the light source.

2.2 PE-ACO-OFDM Rx

Fig. 4 shows the block diagram of the PE-ACO-OFDM Rx. Following optical detection, the received signal is $\boldsymbol{y(t)} = \boldsymbol{r(t)} + w_n(t)$, where $\boldsymbol{r(t)} = R\boldsymbol{p(t)} \circledast h(t)$, R is the responsivity of the photodiode, $\boldsymbol{p(t)}$ is the transmitted optical signal, $h(t)$ is the impulse response and $w_n(t)$ is the shot and terminal noises that are modeled as an AWGN (Additive White Gaussian Noise). However, for the sake of simplicity and without loss of generality, the impulse response and the photodiode responsivity are assumed to be ideal (i.e., $R = h(t) = 1$). The signal $\boldsymbol{y(t)}$ is then passed through the LPF before being fed to the ADC (Analog-to-Digital Conversion) unit and CP removal modules. Next, the resulting signal $\boldsymbol{yc}$ is fed to a separator module to separate the received inverted data samples $\boldsymbol{ya}$ (i.e., $\boldsymbol{xa}$ with noise) from the encoded data samples $\boldsymbol{ye}$ (i.e., $\boldsymbol{xe}$ with noise). Subsequently, $\boldsymbol{ye}$ is fed to the encoded ACO-OFDM demodulator in order to regenerate the encoded binary bit stream $\boldsymbol{bc}$. The inverted negative samples of $\boldsymbol{ya}$ are then assigned their negative values with respect to $\boldsymbol{bc}$, with the resultant signal given as

$$yd_J = \begin{cases} ya_J, & \text{if } bc_J = 0, \\ -ya_J, & \text{if } bc_J = 1, \end{cases} \tag{3}$$

where J is the Jth sample and Jth bit of $\boldsymbol{yd}$ and $\boldsymbol{bc}$ respectively (i.e., $J = \{0, 1, 2, 3, \cdots, N/2 - 1\}$).

Finally, the transmitted data bit stream is reconstructed by applying $\boldsymbol{yd}$ to the ACO-OFDM demodulator.

3 PE-ACO-OFDM data rates

Following the removal of anti-symmetric and negative inversion processes, $\boldsymbol{xc}$ will have $N/2$ number of samples (Fig. 3(d)). However, because of the requirement for additional encoding processes in this work (Fig. 1), $\boldsymbol{xc}$ is combined with $\boldsymbol{xe}$ (Fig. 3(f)). Thus, the total number of samples in PE-ACO-OFDM, N_{PE}, which are required to transmit the same ACO-OFDM data symbol, is given by

$$N_{\text{PE}} = \frac{N}{2} + \frac{2N}{L_e} = \frac{(4 + L_e)N}{2L_e}. \tag{4}$$

Tab. 1 lists the N_{PE} required for transmitting the same ACO-OFDM data symbol, for a range of L_e.

Table 1 Required N_{PE} for a range of L_e

L_e	required N_{PE}
2	1.5 N
4	N
5	0.9 N
6	0.83 N
7	0.78 N
8	0.75 N
9	0.723 N
10	0.7 N

From Eq. (4) and Tab. 1, it can be clearly observed that:

$$\begin{cases} N_{\mathrm{PE}} < N \text{ for } L_e > 4, \\ N_{\mathrm{PE}} \geqslant N \text{ for } L_e \leqslant 4. \end{cases} \tag{5}$$

In general, for ACO-OFDM with no CP, the data rate is given by[25]

$$R^{\{\mathrm{ACO}\}_d} = \frac{DBL}{N}, \tag{6}$$

where B is the available bandwidth, $L = \mathrm{lb}M$, and M is the data constellation order for OFDM. Subsequently, the data rates for PE-ACO-OFDM are given by

$$\begin{aligned} R^{\{\mathrm{PE\text{-}ACO}\}_d} &= \frac{DBL}{N_{\mathrm{PE}}} = \frac{2L_e}{4+L_e}\frac{DBL}{N} \\ &= \frac{2L_e}{4+L_e} R^{\{\mathrm{ACO}\}_d}. \end{aligned} \tag{7}$$

From Eq. (7), it can be seen that $R^{\{\mathrm{PE\text{-}ACO}\}_d}$ increases with L_e. In addition, $R^{\{\mathrm{PE\text{-}ACO}\}_d} \gg R^{\{\mathrm{PE\text{-}ACO}\}_d}$ for $L_e \gg 4$.

The percentage increase in R_d as a function of L_e for the proposed scheme when compared with the traditional ACO-OFDM is defined by Eq. (8) and illustrated in Fig. 5.

$$R^{\{\mathrm{inc}\}_d} = \frac{R^{\{\mathrm{PE\text{-}ACO}\}_d}}{R^{\{\mathrm{PE\text{-}ACO}\}_d}}\% = \frac{2L_e}{4+L_e}\%. \tag{8}$$

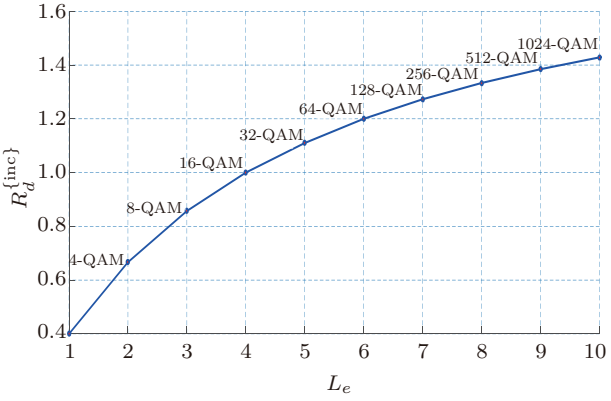

Figure 5 Percentage increase in the data rate vs. L_e, for PE-ACO-OFDM relative to ACO-OFDM

4 PE-ACO-OFDM orthogonality

The orthogonality of the proposed PE-ACO-OFDM signal is mathematically established by showing how the ACO-OFDM signal is still orthogonal after removing its second half. Referring to Fig. 1, the output of the IFFT is an ACO-OFDM signal which is given by

$$x_k = \frac{1}{N}\sum_{i=0}^{N-1} X_i \exp\frac{\mathrm{j}2\pi ik}{N}, \tag{9}$$

where $k = \{0,1,2,3,\cdots,N-1\}$ and $i = \{0,1,2,3,4,\cdots,N-1\}$ are the kth ACO-OFDM sample in the time domain and the ith ACO-OFDM subcarrier in the frequency domain. Following the removal of the second part of ACO-OFDM, the resulting signal is described as

$$\boldsymbol{xa} = \left\{xa_0, xa_1, xa_2, \cdots, xa_{(Z-1)}\right\}, \tag{10}$$

where $Z = N/2$. However, $\boldsymbol{xa}$ is an orthogonal signal if the integration of the products of its frequency domain signal ($\boldsymbol{XA}$) is zero, as given by:

$$XA_n = \sum_{m=0}^{Z-1} X_m \exp\frac{-\mathrm{j}2\pi nm}{Z}, \tag{11}$$

where $n = \{0,1,2,3,4,\cdots,Z-1\}$. Then, the integration of the products of $\boldsymbol{XA}$ can be expressed as

$$\sum_{n=0}^{Z-1} XA_n = \sum_{m=0}^{Z-1} X_m \sum_{n=0}^{Z-1} \exp\left(\frac{-\mathrm{j}2\pi nm}{Z}\right)$$

$$
\begin{aligned}
&= \sum_{m=0}^{Z-1} X_m \sum_{n=0}^{Z-1} \exp\left(\frac{-\mathrm{j}2\pi m}{Z}\right)^n \\
&= \sum_{m=0}^{Z-1} X_m \frac{1-\left(\exp\left(\frac{-\mathrm{j}2\pi m}{Z}\right)\right)^Z}{1-\exp\left(\frac{-\mathrm{j}2\pi m}{Z}\right)} \\
&= \sum_{m=0}^{Z-1} X_m \frac{1-\exp\left(-\mathrm{j}2\pi m\right)}{1-\exp\left(\frac{-\mathrm{j}2\pi m}{Z}\right)} \\
&= 0, \quad m = 0, 1, 2, 3, \cdots, Z-1. \qquad (12)
\end{aligned}
$$

5 Simulation results

In the simulation, $h(t)$ and R were both assumed to be ideal, both the shot and thermal noise sources were modeled as AWGN, and there were 512 IFFT points. Because of the HS and the odd modulation requirements for PE-ACO-OFDM and ACO-OFDM, only 128 subcarriers were modulated. However, owing to the same reason and because the bit loading was not implemented in this simulation study, we only considered 256-QAM (i.e., $L_e = 8$) for PE-ACO-OFDM. All of the key system parameters adopted in the simulation are listed in Tab. 2.

Table 2 Simulation parameters

parameter	value
LED bandwidth	4 MHz
1st order low pass filter	4 MHz
IFFT points	512
transmitted data symbol	128
data symbol length	8, 9, 10
number of frames	1 000 000
modulation type and order	256, 512 and 1 024 QAM for ACO-OFDM and only 256-QAM for PE-ACO-OFDM
encoded modulation order	256 QAM
channel	ideal and AWGN

Fig. 6 shows the BER (Bit Error Rate) as a function of the SNR over an AWGN channel for PE-ACO-OFDM and for the traditional ACO-OFDM. Here, only 256-QAM was considered for PE-ACO-OFDM while 256-, 512- and 1 024-QAM were considered for ACO-OFDM. The figure shows that for a BER of 10^{-3} (i.e., the forward error correction limit), the SNR requirement for the proposed PE-ACO-OFDM is 30 dB compared with 29 dB, 32 dB, and 35 dB for 256-, 512-, and 1 024-QAM ACO-OFDM, respectively. The proposed PE-ACO-OFDM only requires an additional 1 dB of SNR compared with 256-QAM ACO-OFDM. This is because any errors generated during the negative inversion process at the PE-ACO-OFDM Rx affect all PE-ACO-OFDM subcarriers in the frequency domain.

Next we investigated the system throughput, where only the received corrected bits were divided by every OFDM symbol duration, for a range of SNR values. Fig. 7 shows the data throughput against SNR for 256-QAM PE-ACO-OFDM and 256-, 512-, and 1 024-QAM ACO-OFDM. The figure shows that the throughput gradually increases with SNR, reaching the saturation level beyond SNR values of approximately 29, 31, 34, and 30 dB for 256-, 512-, and 1 024-QAM ACO-OFDM and 256-QAM-PE-ACO-OFDM, respectively. Furthermore, the figure also shows that 256-QAM PE-ACO-OFDM offers an increase in the data throughput of approximately 13.2, 8.2, and, 3.2 Mbit/s compared with 256-, 512-, and 1 024-QAM ACO-OFDM, respectively. This is because the symbol duration of 256-QAM PE-ACO-OFDM is reduced by 25%. This improvement in the data throughput compensates for the additional 1 dB SNR requirement in PE-ACO-OFDM compared with 256-QAM-ACO-OFDM.

6 Conclusion

A new PE-ACO-OFDM scheme in IM/DD-based VLC systems was introduced in this paper to enhance the data transmission rate of traditional ACO-OFDM. This was achieved by reducing the symbol duration of the ACO-OFDM signal, by removing the second half of its anti-symmetric time domain signal, while the negative samples of the first half were inverted to meet the requirement for a real and positive signal in IM/DD VLC systems. Additional encoded ACO-OFDM samples were implemented and com-

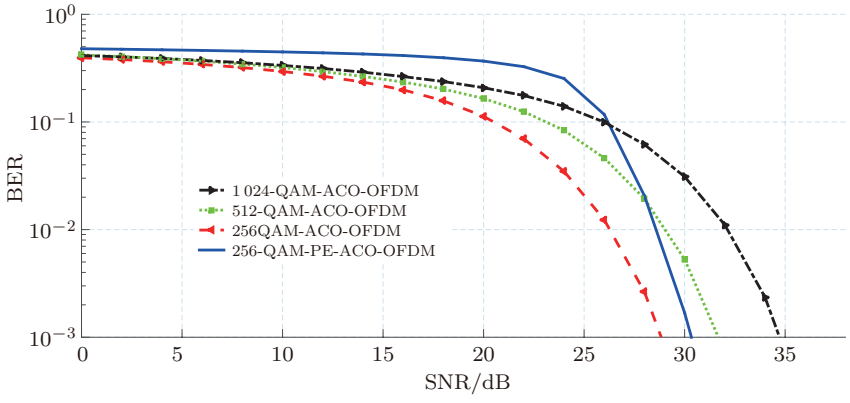

Figure 6 BER against SNR for PE-ACO-OFDM and ACO-OFDM for a range of QAM

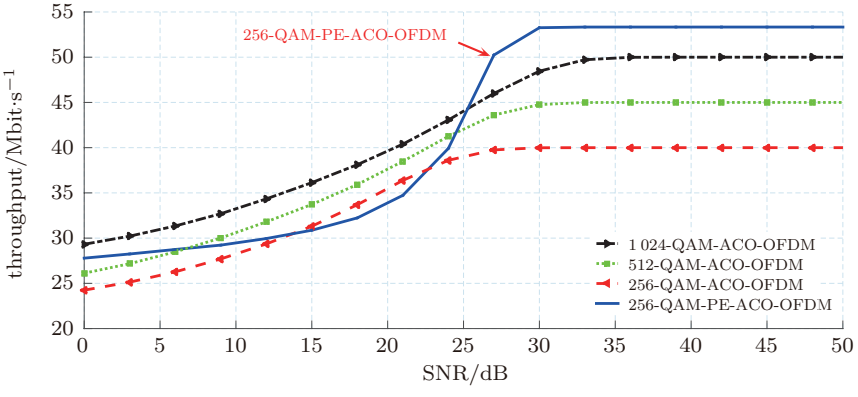

Figure 7 Throughput against the SNR for 256-, 512- and 1 024-QAM ACOO-OFDM and 256-QAM PE-ACO-OFDM

bined with every OFDM symbol, to allow the Rx to identify the positions of the inverted samples. Simulation results showed that PE-ACO-OFDM offered a 33% increase in the data throughput compared with 256-QAM-ACO-OFDM. However, this was achieved at the cost of the SNR increasing by 1 dB, compared with ACO-OFDM.

References

[1] Z. Ghassemlooy, W. Popoola, S. Rajbhandari. Optical wireless communications: system and channel modelling with Matlab [M]. London, UK: CRC Press, 2013.

[2] Z. Ghassemlooy, L. N. Alves, S. Zvanovec, et al. Visible light communications: theory and applications [M]. London, UK: CRC Press, 2017.

[3] J. Grubor, S. C. J. Lee, K. D. Langer, et al. Wireless high-speed data transmission with phosphorescent white-light LEDs [C]//33rd European Conference and Exhibition of Optical Communications, 2007: 1-2.

[4] S. W. Wang, F. L. Chen, L. Y. Liang, et al. A high-performance blue filter for a white-led-based visible light communication system [J]. IEEE wireless communications, 2015, 22(2): 61-67.

[5] P. A. Haigh, Z. Ghassemlooy, S. Rajbhandari, et al. Visible light communications: 170 Mb/s using an artificial neural network equalizer in a low bandwidth white light configuration [J]. Journal of lightwave technology, 2014, 32(9): 1807-1813.

[6] X. X. Huang, J. Y. Shi, J. H. Li, et al. A Gb/s VLC transmission using hardware pre-equalization circuit [J]. IEEE photonics technology letters, 2015, 27(18): 1915-1918.

[7] H. L. Minh, D. O. Brien, G. Faulkner, et al. High-speed visible light communications using multiple-resonant equalization [J]. IEEE photonics technology letters, 2008, 20(14): 1243-1245.

[8] K. Burse, R. N. Yadav, S. C. Shrivastava. Channel equalization using neural networks: a review [J]. IEEE transactions on systems, man, and cybernetics, Part C (Applications and Reviews), 2010, 40(3): 352-357.

[9] F. Jiuchao, C. K. Tse, F. C. M. Lau. A neural-network-based channel-equalization strategy for chaos-based communication systems [J]. IEEE transactions on circuits and systems I: fundamental theory and applications, 2003, 50(7): 954-957.

[10] J. Vucic, C. Kottke, S. Nerreter, et al. 513 Mbit/s visible light communications link based on DMT-modulation of a white LED [J]. Journal of lightwave technology, 2010, 28(24): 3512-3518.

[11] Y. S. Cho, J. Kim, W. Y. Yang, et al. MIMO-OFDM wireless communications with Matlab [M]. Hoboken, NJ: Wiley, 2010.

[12] M. S. Islim, H. Haas. Modulation techniques for Li-Fi [J]. ZTE communications, 2016, 14(2): 29-40.

[13] A. M. Khalid, G. Cossu, R. Corsini, et al. 1-Gb/s transmission over a phosphorescent white LED by using rate-adaptive discrete multi-tone modulation [J]. IEEE photonics journal, 2012, 4(5): 1465-1473.

[14] D. Tsonev, H. Chun, S. Rajbhandari, et al. A 3-Gb/s single-LED OFDM-based wireless VLC link using a gallium nitride μLED [J]. IEEE photonics technology letters, 2014, 26(7): 637-640.

[15] G. Cossu, A. Khalid, P. Choudhury, et al. 3.4 Gbit/s visible optical wireless transmission based on RGB LED [J]. Optics express, 2012, 20(26): 501-506.

[16] F. M. Wu, C. T. Lin, C. C. Wei, et al. Performance comparison of OFDM signal and CAP signal over high capacity RGB-LED-based WDM visible light communication [J]. IEEE photonics journal, 2013, 5(4): 7901507.

[17] A. H. Azhar, T. Tran, D. O'Brien. A gigabit/s indoor wireless transmission using MIMO-OFDM visible-light communications [J]. IEEE Photonics technology letters, 2013, 25(2): 171-174.

[18] J. B. Carruthers, J. M. Kahn. Multiple-subcarrier modulation for nondirected wireless infrared communication [J]. IEEE journal on selected areas in communications, 1996, 14(3): 538-546.

[19] J. Armstrong, A. J. Lowery. Power efficient optical OFDM [J]. Electronics letters, 2006, 42(6): 370-372.

[20] S. D. Dissanayake, J. Armstrong. Comparison of ACO-OFDM, DCO-OFDM and ADO-OFDM in IM/DD systems [J]. Journal of lightwave technology, 2013, 31(7): 1063-1072.

[21] J. Armstrong, B. Schmidt, D. Kalra, et al. Performance of asymmetrically clipped optical OFDM in AWGN for an intensity modulated direct detection system [C]//IEEE Global Telecommunications Conference, GLOBECOM, 2006: 1-5.

[22] S. D. Dissanayake, K. Panta, J. Armstrong. A novel technique to simultaneously transmit ACO-OFDM and DCO-OFDM in IM/DD systems [C]//IEEE Global Telecommunications Conference, Workshops, 2011: 782-786.

[23] F. Yang, J. N. Gao, S. C. Liu. Novel visible light communication approach based on hybrid OOK and ACO-OFDM [J]. IEEE photonics technology letters, 2016, 28(14): 1585-1588.

[24] O. Saied, Z. Ghassemlooy, X. W. Dai, et al. Pilot-aided asymmetrically clipped optical OFDM in visible light communication [J]. The mediterranean journal of electronics and communications, 2016, 12(2): 64-71.

[25] R. Mesleh, H. Elgala, H. Haas. On the performance of different OFDM based optical wireless communication systems [J]. IEEE/OSA journal of optical communications and networking, 2011, 3(8): 620628.

About the authors

Osama Saied received his higher diploma degree in electronic engineering from the High Institute for Poly-Technics, Gharyan, Libya in 2000, worked as networking engineering from 2001 to 2008 in Biruni Remote Sensing Center (BRSC) Tripoli, Libya. He received his M.Sc. degree in communication and signal processing in 2010, University of Newcastle upon Tyne, U.K.. He has been doing his Ph.D. in visible light communications at Northumbria University, Newcastle upon Tyne, U.K., since 2013. (Email: osama.saied@northumbri.ac.uk)

Zabih Ghassemlooy received his B.Sc. degree (Hons.) in electrical and electronics engineering from Manchester Metropolitan University, Manchester, U.K., in 1981, and the M.Sc. and Ph.D. degrees from the Institute of Science and Technology, Manchester, University of Manchester, U.K., in 1984 and 1987, respectively. From 1987 to 1988, he was a post-doctoral research fellow with City University, U.K.. In 1988 he joined Sheffield Hallam University as a lecturer, becoming a reader in 1995 and became a professor in optical communications in 1997. In 2004 he joined the University of Northumbria (UNN), Newcastle, as an associate dean (AD) for research with the School of Computing, Engineering, and Information Sciences, and from 2012 to 2014, he was an AD of Research and Innovation, Faculty of Engineering, UNN, U.K., where he currently is the head of the Northumbria Communications Research Laboratories. In 2001 he was awarded the Tan Chin Tuan Fellowship in Engineering from the Nanyang Technological University in Singapore. In 2016 he became a research fellow at the Chinese Academy of Sciences, and since 2015 he has been a distinguished professor with the Chinese Academy of Sciences, Quanzhou, China. He is a visiting professor at the University Tun Hussein Onn Malaysia, Malaysia (2013-2017), and Huaqiao University, Quanzhou, China (2017-2018). He published over 690 papers (258 journals and 6 books), over 88 keynote and invited talks, and supervised 57 Ph.D. students. His research interests include optical wireless communications, free space optics, and visible light communications. He was the vice-chair of EU Cost Action IC1101 (2011-2016). He is the chief editor of the British journal of applied science and technology and the International journal of optics

and applications. He is a fellow of the IET, a senior member of IEEE, and a member of OSA. He is a co-author of a CRC book on "Optical Wireless Communications—Systems and Channel Modelling with Matlab (2012)"; and co-editor of four books including the Springer book on "Optical Wireless Communications—An Emerging Technology (2016)", CRC book on "Visible Light Communications: Theory and Applications, CRC June 2017", IGI Global book on "Intelligent Systems for Optical Networks Design: Advancing Techniques, 31 Mar 2013", and IET book on "Analogue Optical Fibre Communications, IEE Telecommunication series 32, 1995". From 2004-2006 he was the IEEE UK/IR Communications chapter secretary, the vice-chairman (2004-2008), the chairman (2008-2011), and chairman of the IET Northumbria Network (Oct. 2011-2015). (Email: z.ghassemlooy@northumbria.ac.uk)

Xuan Tang is an academic leader and professor at the Fujian Institute of Research on the structure of matter, Chinese Academy of Sciences (CAS). She is a team member of Youth Innovation Promotion Association CAS. Her research interests are in the areas of optical wireless communication systems including high speed infrared/ultraviolet laser communications, visible light communications and optical MIMO systems, as well as radio frequency communication technologies. In June 2008 she was awarded BEng (1st Class with Hons.) in electronic and communications engineering from Northumbria University, Newcastle, U.K.. In 2013 she obtained her Ph.D. degree on polarisation shift keying modulated free-space optical communication systems, and it was in collaboration with Chosun University, South Korea. From Oct. 2012 to Jul. 2014, she worked as the postdoctoral researcher at the Department of Electronic Communications Engineering, Tsinghua University. From Oct. 2013 to Apr. 2014, she was a visiting academic at University of Science and Technology of China. Her group has obtained 13 funds, including General Financial Grant from China Postdoctoral Science Foundation, National Science Fund for Young Scholars, External Cooperation Program of Chinese Academy of Sciences, Youth Innovation Promotion Association CAS, Returned Overseas Chinese Scholars of the State Education Ministry and so on, the grant of which is as much as ten-million yuan. She has published over 50 papers, of which almost 30 are SCI papers. She acts as a reviewer for a number of high impact journals including IEEE journal of lightwave technology, IEEE journal on selected areas in communications, IET communications, applied optics, etc. (Email: xtang@fjirsm.ac.cn)

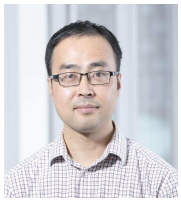

Xuewu Dai received his B.Eng. degree in communication engineering and M.Sc. degree in computer science from Southwest University, China, respectively, and a Ph.D. degree in electrical and electronic engineering from the University of Manchester, U.K., 2008. Prior to his appointment at Northumbria University, he did post-doctoral research at University of Oxford (2011-2013) and University College London (2009-2011), respectively. His research covers both academic and industrial interests, centered around the robust state estimation and its applications to condition monitoring, OFDM channel estimation, wireless sensor actuator networks. He has published over 40 research articles in peer-reviewed journals and world-leading conferences, and served as regular reviewers for some top journals and as TPC members for several IEEE conferences (such as ICC'2015/2016, etc). (Email: xuewu.dai@northumbria.ac.uk)

Hoa Le Minh received his B.Eng. degree in telecommunications in 1999 at Bach Khoa University of Hochiminh city, Vietnam, and then worked as lecturer in Telecommunications Department at the same University. He received M.Sc. degree in 2003 and in 2007 his Ph.D. degree in telecommunications in Munich University of Technology (TUM), Germany and Northumbria University, Newcastle, U.K., respectively. Hoa worked as a research assistant in Siemens AG, Munich, Germany during 2002-2004 and postdoctoral research fellow in University of Oxford, U.K., from 2007 to 2010. Since 2010 he has been the senior lecturer at Northumbria University. His research areas are wireless communications, optical wireless communications, sensor network and smartphone technology. He has published over 150 papers in these fields. Currently he is chairman of IEEE ComSoc U.K. and Ireland. (Email: hoa.leminh@northumbria.ac.uk)

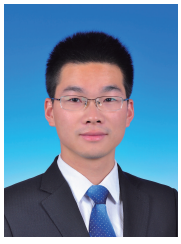

Bangjiang Lin received his B.S. and Ph.D. degrees from Electronics Engineering Department of Peking University, Beijing, China, in 2010 and 2015, respectively. He is currently working as an associate professor in Quanzhou Institute of Equipment Manufacturing, Haixi Institutes, Chinese Academy of Sciences. His research interests include passive optical network, visible light communications. (Email: linbangjiang@163.com)